

Quasiparticle electronic structure of charged oxygen vacancies in TiO₂

Ali Kazempour, Javad Hashemifar, and Hadi Akbarzadeh

Department of Physics, Isfahan University of Technology, Isfahan 84156-83111, Iran

Abstract

We studied the oxygen vacancies (V_O) in rutile TiO₂ by using G_0W_0 approximation on top of GGA+ U as a method of choice to improve the gap. Since there is no extensive agreement regarding the characteristic of electron localization for TiO_2 , we examine combined $G_0W_0@GGA+U$ scheme in which both are conceptually one step toward better enumeration of the non locality of exchange-correlation potential. Our $G_0W_0@GGA+U$ results realize and confirm the weak nature of electron correlation in rutile TiO_2 and shows that the U -dependence of the energy gap in perfect bulk is slightly stronger than in defected sample. In addition, we studied the U -dependency of V_O defect states and found that different charged vacancies shows different U -dependence. While the application of G_0W_0 correction would improve the quasiparticle gap and formation energies, however the V_O states, in contrast to experiment, remains entangled with the conduction band. Finally, we used PBE0 and HSE06 hybrid functionals and found that these exchange-correlation functional particularly HSE06 that reproduced the real gap and provide desire description of the screening, properly disentangle the neutral and singly ionized V_O from the conduction band. According to hybrid functional calculations, all vacancies are stabilized and V_O with 2+ charge state is the most stable vacancy in the whole Fermi-level range inside the gap and hence V_O acts as a shallow donor.

PACS numbers:

TiO_2 has attracted many interests with application as photo catalysis, water splitting, solar cell and sensors^{1,2}. It has been demonstrated that TiO_2 can be reduced easily and reach high degree of nonstoichiometry which leads to high n-type conductivity³. With thermal excitation, oxygen vacancy (V_O) may loose its electrons and becomes charged. Some thermogravimetric measurements reported that the electrical conductivity demonstrate various scaling as a function of oxygen partial pressure and temperature . Each scaling behavior correspond to the dominance of solely one vacancy charge state³. On the other hand , there are experimental findings that shows rather dominance of Ti interstitial and independent picture of conductivity in terms of oxygen partial pressure⁴. On the theoretical side,several investigations have been performed from embedded cluster to ab-initio total energy methods on the oxygen-deficient rutile TiO_2 sample.⁵⁻⁷. Cho et al.⁶ using local-density approximation (LDA) observed the entangled V_O state inside conduction band. Park et al.⁸ in an alternative ab-initio study using Hubbard correction for both $Ti - 3d$ and $O - 2p$ were only able to locate V_O^+ below conduction band minimum about 1 eV . But it doesn't give the neutral vacancy V_O^0 state in the gap. Moreover both above mentioned theoretical studies suffer from the band gap underestimation. In spite of wide research on rutile including the role of V_O in n-type electrical conductivity, its localized nature is still under debate. Therefore it seems necessary to reinvestigate the features of V_O in TiO_2 . Although Density Functional Theory has been regarded as a valuable tool for microscopic understanding of defect mechanisms, but the inadequate description of self-energy and underestimation of energy gap in popular local density (LDA) and generalized gradient approximation (GGA) leads to a widespread deficiencies. These limitations lead to artificial characterization of defect states and wrong position of thermodynamic transition levels. It is believed that overcoming gap problem leads to reliable determination of defect states motivated using methods such as DFT+ U , Hybrid functionals and Self-interaction correction to partly improve the self-interaction. Qualitatively, Many Body Perturbation Theory (MBPT) in the GW approach has shown successful treatment of quasi-particles band structure in semiconductors and is considered as a promising method to study defects⁹. However, application of GW on systems with partially filled d or f orbital due to wrong-predicted LDA band ordering yield unreliable electronic spectra and the dependence of spectra on adjustable parameters or starting point remain involved¹⁰. Alternatively, LDA or GGA starting point might be substituted with one giving closer features to respective QP band energies. As a benchmark, we choose GGA+ U

single-particle solution as starting point in GW scheme to evaluate problematic positioning of V_O in reduced TiO_{2-x} . Moreover, this choice may provide insightful information about localized nature of the V_O states. Our results show smoothly U -dependence of vacancy affinity all are greater than CBM affinity and therefore $G_0W_0@GGA+U$ fails to stabilize V_O^0 and V_O^+ inside the gap. Additionally, in the realm of post-DFT methods, we employ Hybrid functionals PBE0 and HSE in which they partially reduce self-interaction errors and improve gap in the description of vacancy states. The obtained results show that V_O acts as a shallow donor with V_O^{2+} being the most stable charge in the whole variation of Fermi level.

I. COMPUTATIONAL DETAILS

The calculations are performed using $GGA+U$ based on PBE formalism for generalized gradient approximation¹¹ as starting point for G_0W_0 and PBE0 and HSE06 exchange-correlation functional with a plane wave basis set and norm-conserving pseudopotentials. Atomic orbitals 3s, 3p, 4s, and 3d are included into the Ti valence subspace, while 3s and 3p orbitals are considered as valence for O. Spin-polarized calculation are considered for systems with an odd number of electrons. The cutoff energy 70 Ryd was chosen based on convergence of the cohesive energy of rutile TiO_2 and for Brillouin zone integration we use a mesh of $2 \times 2 \times 2$. To remove the interaction of neighboring supercell we performed 72, 96 and 108 atoms supercell calculations in which the difference between 72 and 96 atoms supercell defect formation energy is less than 0.02 eV and 0.04 eV for neutral and charged vacancies and therefore choose 72 atoms supercell. All defected supercells are fully relaxed until the forces are below 1 mRyd/bohr. In $GGA+U$, the value of the Hubbard term U , applied to the Ti 3d states, is varied between 0 and 4 eV. This range was chosen based on the estimate of the value of U obtained using a constrained GGA calculation, as implemented in the QUANTUM ESPRESSO code¹², and also by calculating U for an isolated Ti atom, divided by the theoretical optical dielectric constant $\epsilon_\infty = 6.7$. Both approaches give similar U values of about 1.2 eV. The GW approach is applied non-self-consistently (G_0W_0), exploiting the first order expansion of the self-energy^{13,14}. The dynamic behavior of the dielectric matrix is determined by the plasmon-pole approximation as implemented in the SAX code¹⁵. The defect formation energies are calculated according to

$$E^f[X_q] = E_{\text{tot}}[X_q] - E_{\text{tot}}[\text{bulk}] + \mu_O + q[E_F + E_{\text{VBM}} + \Delta V] \quad (1)$$

where $E_{\text{tot}}[X_q]$ and $E_{\text{tot}}[\text{bulk}]$ are defected and perfect supercell total energy, respectively. The reference for the oxygen chemical potential is chosen to be $1/2EO_2$, while for Ti the chemical potential is referenced to the bulk Ti. The electronic chemical potential(Fermi energy) is referenced to the valence band maximum (VBM) corrected by the alignment of the electrostatic potential in perfect and defect supercell far enough from defect states. Moreover, in Charged cases, the Makov-Payne correction¹⁶ have not been included due to large dielectric constant entering in Madelung term.

II. $G_0W_0@GGA+U$ METHODOLOGY

It was argued that $GGA+U$ can be viewed as an approximation to GW for localized d and f states¹⁷. However, due to U correction on localized states, the hybridization of localized states with others has not been included i.e. the itinerant states remain at GGA level that in some cases isn't true. Moreover, in $GGA+U$, the double counting (in the $LDA+U$ formalism, double counting removes a part of electron-electron interaction that was already included in LDA Hamiltonian) term is not well defined. On the other hand screening is described statically while in fact it behaves dynamically and has strong energy dependence for particularly localized electrons. Furthermore it was shown that for open-shell and shallow d systems the application of G_0W_0 on GGA doesn't yield fine QP band structure attributed to wrong GGA-derived band ordering¹⁸. One solution here is to replace the GGA with $GGA+U$ method which its eigenvalues and eigenfunctions are relatively closer to QP electronic structure^{19,20}. Despite $GGA+U$, G_0W_0 calculation based on $GGA+U$ has not shown U -dependence explicitly while the resulted QP state would show implicit U -dependence²⁰. In the formalism of $GGA+U$ based G_0W_0 ²⁰, the QP equation is expressed as:

$$\varepsilon_i \approx \epsilon_i^{ks} + Z_i \langle \phi_i^{ks} | \Sigma(\epsilon_i^{ks}) - V_{xc} - V_{db} | \phi_i^{ks} \rangle \quad (2)$$

which V_{db} accounts for double counting term. The $GGA+U$ single particle equation is:

$$\epsilon_i^{ks} = \langle \phi_i^{ks} | -\frac{1}{2}\nabla^2 + V_{GGA} + V_{db} | \phi_i^{ks} \rangle = \bar{\epsilon}_i^{ks} + \langle \phi_i^{ks} | V_{db} | \phi_i^{ks} \rangle \quad (3)$$

where $\bar{\epsilon}_i$ can be considered as GGA energies obtained with $GGA+U$ wave function. Eventually, with linear expansion of self-interaction operator $\Sigma(\epsilon_i^{ks})$ around $\bar{\epsilon}_i$ the QP equation

can be written as:

$$\varepsilon_i = \bar{\varepsilon}_i^{ks} + Z'_i \langle \phi_i^{ks} | \Sigma(\bar{\varepsilon}_i^{ks}) - V_{xc} | \phi_i^{ks} \rangle \quad (4)$$

which clearly demonstrate advantage of having no double counting term . Regarding the first term, U correction affects not only the energies of the levels, but also the hybridization between the orbitals, if allowed by symmetry. The most pronounced modification are expected to appear near the Fermi level, where a significant change in localization of electronic states can occur. The states deeper in energy are already quite localized and atomic-like, so that a non-zero U would mostly result to a shift in their energies. In this case, the localized d or f occupied (unoccupied) states are pushed toward lower (higher) energies and get more localized. But the situation for half-filled states are quite demanding and severely depends on the nontrivial hybridization of included orbital as a function of U and it's character. The second term would results in screening alteration and get tendency to increase energy gap with U addition. In general both terms of above equation have contributed into U -dependence of the system in $GW@GGA+U$ scheme.

III. RESULTS AND DISCUSSION

A. A.GW@GGA+U

In previous section , we reviewed the application of $GW@GGA+U$ to determine the affinity and ionization energy i.e. band gap of the perfect system in which the CBM is fully empty. In the case of defected sample which defect-induced state lies inside the gap or in resonance with band edges, the situation slightly changed so that the highest occupied states might be the defect state (in the case the defect states falls inside the gap) or CBM (in which the defect states is in resonance or above CB). It was shown that for TiO_2 all charged V_O states becomes merged in CB in GGA or even GGA+ U derived band structure. However, the Motivation here for the choice of GGA+ U is that the application of U would decreases the outward relaxation of vacancy neighbors and enhance their hybridization leads to better description of the defected sample band structure closer to its real quasiparticle spectra.

Prior to studying defected material, it is advantageous to inspect $G_0W_0@GGA+U$ electronic structure of the perfect bulk. Fig.1 shows comparison between GGA+ U , $G_0W_0@GGA+U$ and XAS experimental density of states of bulk TiO_2 ²¹. Experimental

XAS and GGA+ U was aligned at upper valence band edge with G_0W_0 spectrum. The sharp peak of empty $Ti - 3d$ in XAS spectra is situated between its analogous in GGA+ U and G_0W_0 . While the addition of U would enlarge the GGA+ U gap and the $3d$ peak of Ti becomes closer to XAS counterpart, G_0W_0 gives overestimated gap with $3d$ peak gradually goes away from XAS correspondent.

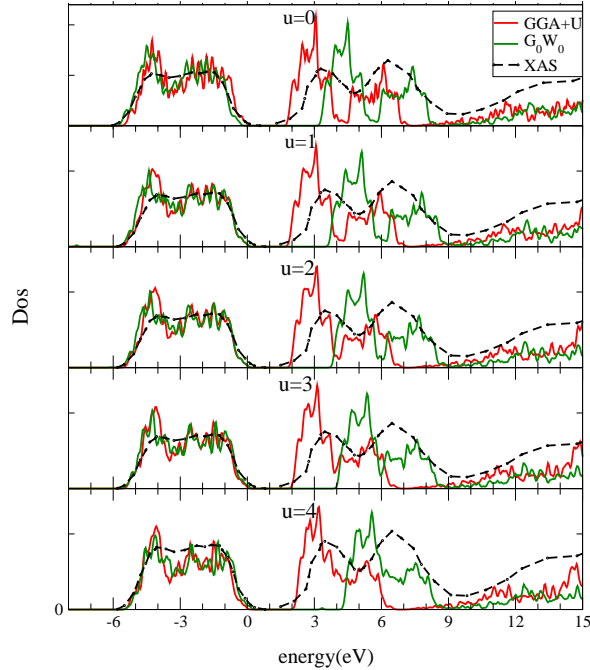


FIG. 1: The Dos of TiO_2 from GGA+ U , $G_0W_0@GGA+U$ and XAS are compared within the range of $U = 0, 4$.

In both GGA+ U and G_0W_0 the most significant correction occurs for CB that are made of $3d$ -Ti via reduction of the conduction band width toward higher energies. As it is shown in Fig.2 the U -sensitivity is more pronounced in G_0W_0 than GGA+ U . The reason could be expressed in response to the question that how much the effect of U change single particle wave-functions and screening in dressed potential that consequently reflect the degree of $p - d$ coupling. It realize that the hybridization of localized orbital with itinerant states that is neglected in GGA+ U , play an important role when combined with G_0W_0 . In other word, the differences in sensitivity of energy gap with U values could be traced back to the augmentation of localized and itinerant hybridization as a function of U . From the inspection of p-d coupling it is evident that smooth behavior of U -sensitivity of the gap confirm the weakly correlated nature of the TiO_2 that already was obtained about 1.2 eV in

previous section. Another useful criteria derives from U dependence of electronic structure is the dimensionless U/W ratio that shows the degree of the localization in TiO_2 typically varies between 0.5-2 for the selected range of $U = 1, 2, 3, 4$ (W is the $3d - Ti$ bandwidth) . By comparison with the typical U/W values obtained for highly correlated material such as NiO which exceed from 4^{20} , it illustrate the weak localization of d-electrons in TiO_2 .

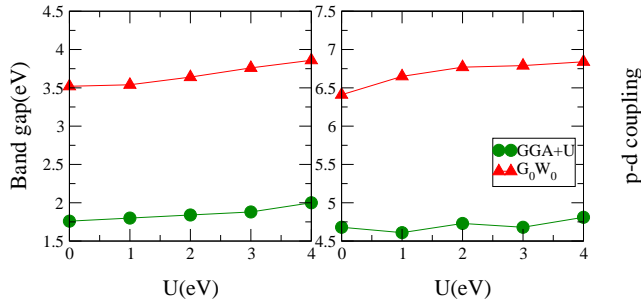


FIG. 2: The values of band gap (left) and the p-d peak distance are shown as a function of U from GGA+ U and $G_0W_0@GGA+U$.

In the case of defect involved TiO_2 , with the addition of U , GGA+ U resulted V_O^0 and V_O^{2+} energy states remain within the conduction band whereas for $U = 2, 3, 4$, V_O^+ state appear below CBM with the values 0.73, 1.12 and 1.73 eV ,respectively. Fig.3 shows the expected downward shift of fully occupied CBM in V_O^0 and half-filled defect states in V_O^+ and upward shift of unoccupied CBM in V_O^+ and V_O^{2+} though the gap problem exist. Having earned the V_O states of GGA+ U , we are able to evaluate the influence of hubbard correction U compared to $GW@GGA+U$ one.

The $G_0W_0@GGA+U$ corrected quasi-particle states are shown for all three charged states of V_O relative to initial GGA+ U in Fig.4. Since the most GW codes does not allow a direct treatment of systems with unpaired electrons, the V_O^+ defect affinity is estimated using the relation $A(+/2+) = I(2 + /+)$ where A and I are affinity and ionization of given defect state for local charge addition. For this reason, we have performed a G_0W_0 calculation with doubly ionized vacancy at the geometry of relaxed V_O^+ . Calculated configuration coordinate diagram is shown in Fig.6 also clearly indicate almost closer configuration of V_O^{2+} and V_O^+ and proximate same values of $I(+/2+)$ at R_+ and R_{2+} . The affinity of the whole of the system was measured relative to upper valence band edge VBM while the affinity of defect states was measured with respect to the lower conduction band CBM. For each V_O , G_0W_0 corrected states shifts up within the conduction band.

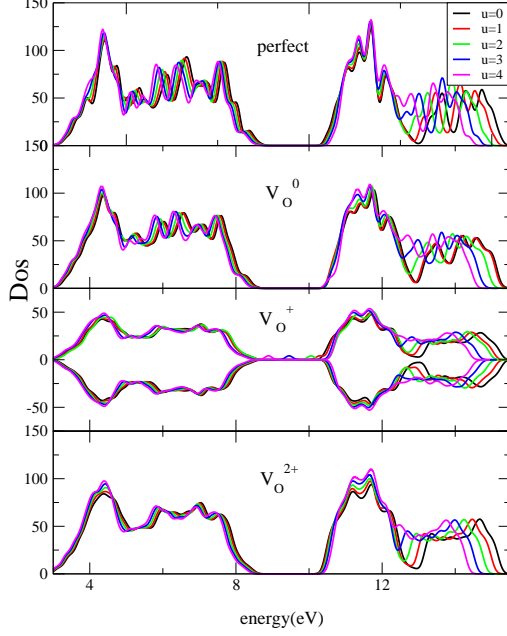


FIG. 3: The effect of U correction on the electronic structure of perfect bulk and different charged oxygen vacancy is compared. For V_O^+ with U addition the defect induced state appear in below CBM.

As a result, it is observed that empty V_O^{2+} and half-filled V_O^+ is more sensitive to the self-interaction correction than filled V_O^0 and the shift of their quasiparticle energies is more remarkable than V_O^0 . Fig. 5 shows the affinity of CBM and vacancy state of V_O^0 and V_O^{2+} species. In $G_0W_0@GGA+U$, the affinity of CBM .i.e band gap for V_O^0 and V_O^{2+} decrease with increasing U within 0.35 eV and 0.20 eV while this values amount to 0.10 eV and 0.15 eV in $GGA+U$, respectively. For the vacancy affinity the resulted values for V_O^0 and V_O^{2+} varies within 0.16 eV and 0.48 eV for G_0W_0 and 0.18 eV and 0.13 eV for $GGA+U$, respectively. Compared to $GGA+U$, it is apparent that the U dependence of G_0W_0 is slightly more for the gap and vacancy affinity. Moreover, the affinity of the oxygen vacancy in both $GGA+U$ and G_0W_0 shows similar linear ascending trend whereas the trend for band gap show inconsistent behavior. Inspection of the quasi-particle correction, shows that the upward shift is more prominent for V_O^{2+} than V_O^0 . This indication illustrate the different characters for vacancy level in which the G_0W_0 application effectively change those states concerned vacancy center with no electrons (with no cost of electrostatic energy). At $U=2$ both vacancies involved concrete change in quasi-particle states. This, however is an artifact of $GGA+U$ that shows new band ordering and the vacancy level crossover some states due

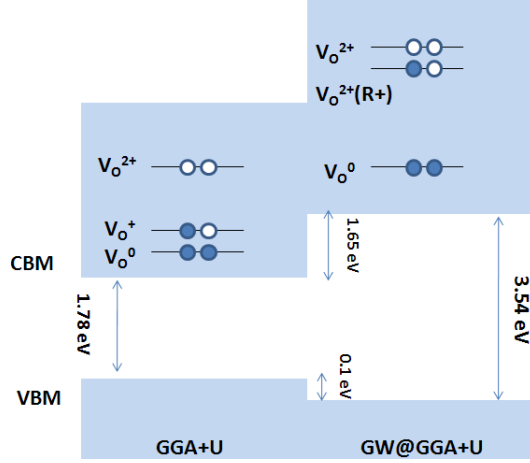


FIG. 4: Single particle GGA+ U (left) and quasi-particle energies (right) for symmetric defect state of various V_O are shown. The self-energy correction would shift up all defect states specially singly and doubly ionized vacancies.

to change in its hybridization..

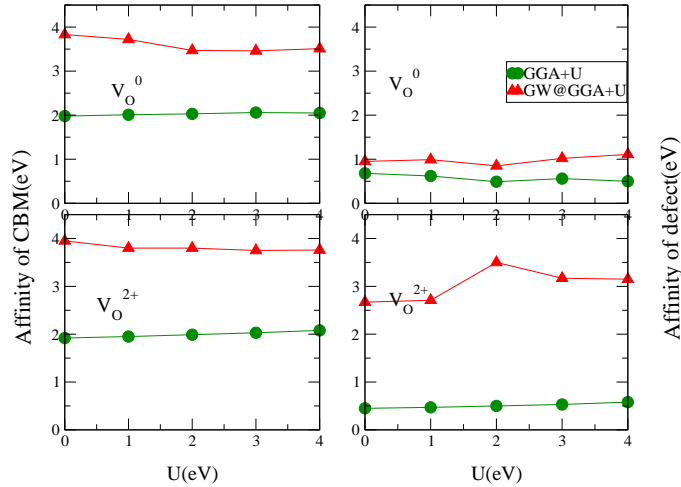


FIG. 5: (left) and (right) represent the comparison of affinity of the whole system and the defect state affinity, for V_O^0 (top) and V_O^{2+} (bottom), respectively.

Using GW correction scheme was proposed by Rinke *et al*²² based on separation of formation energy into local electron addition A and lattice relaxation part Δ , we obtained the corrected formation energy and thermodynamic transition levels. At the first step, the vertical electron affinity between two charged states at fixed geometry is calculated by G_0W_0 formalism. In a second step, the lattice relaxation are measured after charge addition

between initial and final geometries with GGA+ U .(Fig .6)

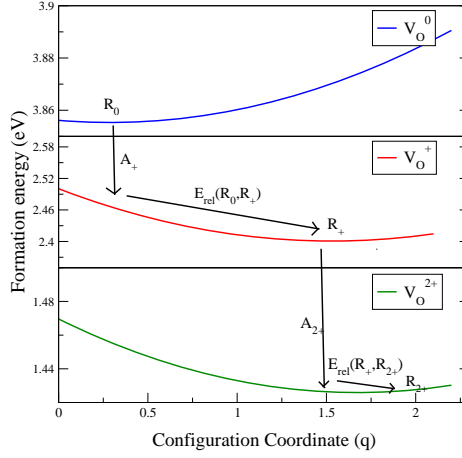


FIG. 6: The simple calculated configuration coordinate diagram with GGA method. Each charged vacancy was computed at three configuration (R_0 , R_+ and R_{2+}). The diagram show closer values of A_{2+} and I_+ for singly and doubly ionized vacancies.

Starting from reference formation energy of V_O^{2+} , the corrected formation energies of V_O^+ and V_O^0 are then given by

$$E_f(+, \epsilon_f) = \Delta(+, R+, R_{2+}) + A(2+, R_{2+}) + E_f(2+, \epsilon_f = 0) \quad (5)$$

and

$$E_f(0, \epsilon_f) = \Delta(+, R0, R+) + A(+, R0) + E_f(+, \epsilon_f = 0) \quad (6)$$

Using calculated affinities for all defects involved we calculated formation energies as a function of U summarized in table.I.

The resulted formation energy for V_O^+ varies within 1.2-2.5 eV and within the rang of 0.15-0.95 eV for V_O^0 as a function of U . The increase of V_O^+ formation energy relative to neutral ones implies that its concentration is now much lower than the GGA+ U counterpart as is shown in Fig.7 . Also affinity of V_O^+ changes inasmuch as its stability as a variation of Fermi level (chemical potential) in the gap is vanished relative to GGA+ U . With U addition, this trend will continue up along with the V_O^{2+} becomes the most covered stable charge in the energy gap and consequently the charged transition level $\epsilon(2+ / 0)$ would shift up though remain inside the gap. Furthermore, the charged transition level $\epsilon(2+ / 0)$ change from 1.70 and 1.89 eV at $U = 1$ up to 1.82 and 2.28 eV at $U = 4$ for GGA+ U and G_0W_0 , Respectively. Hence, although $G_0W_0@GGA+U$ doesn't stabilize V_O^0 and V_O^+ in the gap, it

TABLE I: All corrected formation energies by $GW@GGA+U$ are listed in units of eV. The starting formation energy of V_O^{2+} has been taken from GGA+ U values.

	Δ_2	Δ_1	A(+/0)	A(2+/+)	$E_f(2+)$	$E_f(+)$		$E_f(0)$	
						GGA+ U	G0W0	GGA+ U	G0W0
U=0	0.05	0.01	0.75	2.66	0.66	2.16	3.37	3.98	4.14
U=1	0.25	0.04	0.79	2.71	0.85	2.33	3.81	4.25	4.64
U=2	0.36	0.08	0.67	2.43	1.00	2.41	3.79	4.53	4.54
U=3	0.47	0.10	0.82	2.87	1.22	2.42	4.56	4.88	5.48
U=4	0.55	0.15	0.90	2.96	1.42	2.37	4.93	5.02	5.98

gives V_O^{2+} the most dominant stable vacancy with growing U and eliminate the stability of singly ionized V_O for all fermi-level position within the gap.

B. B.Hybrid functionals, HSE06 and PBE0

We now turn to hybrid functionals that hopefully overcome the band gap problem. While a number of hybrid functional have been introduced²³, we already focus on $PBE0$ and $HSE06$ which typical gap has qualitative agreement with experiment. While recently published study with HSE06 functional gives comprehensive description of oxygen vacancies²⁴, the comparison of HSE06 and PBE0 results gives efficient insight how does the short and long range of exchange interaction affect the defect levels. In principle ,for both PBE0 and HSE06 ,the exchange energy part is taken as

$$E_x^{hyb} = aE_x^{HF} + (1 - a)E_x^{GGA} \quad (7)$$

with $a=0.25$ and the correlation part remains at GGA level except that in the latter the short-range part of the HF exchange potential is kept²⁵.

The reason behind choosing these functionals lies in the fact that they provide improved gap in many materials²⁶. The calculations performed in this section was done with same parameter and accuracy as in previous section. Furthermore, our obtained total energy include singularity correction of the $G=0$ exchange potential . For the perfect TiO_2 bulk the energy gap are 4.15 eV and 3.10 eV for PBE0 and HSE06 ,respectively shows good

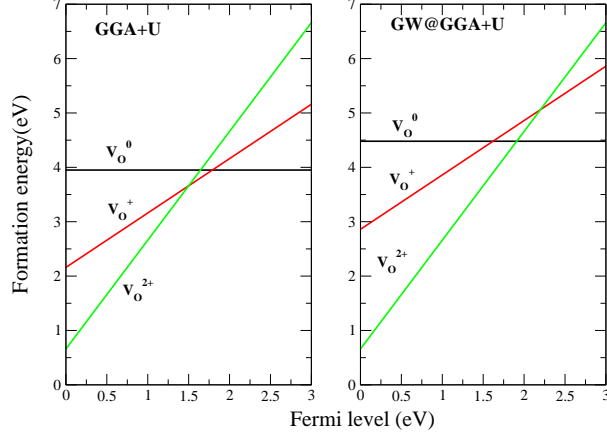


FIG. 7: The comparison between GGA+ U and correction scheme using $G_0W_0@GGA+U$ is shown. G_0W_0 correction method results in metastable V_O^+ with variation of Fermi energy.

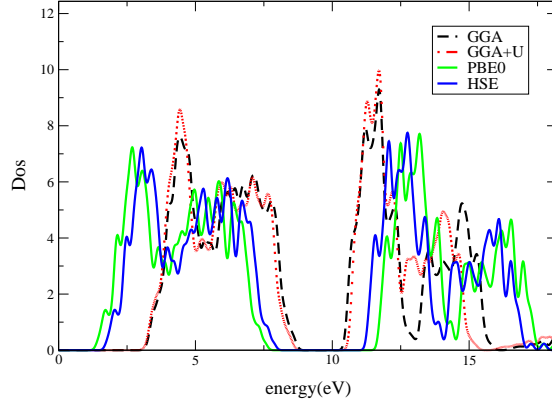


FIG. 8: The DOS of hybrid functionals HSE06 and PBE0 compared to GGA and GGA+ U are plotted. A portion of HF exchange addition in hybrid functionals give raise to gap opening.

agreement of HSE06 gap with experimental value 3.05 eV. The comparison of different functional gap are shown in Fig.8. from inspection of above density of states it seems that the addition of a portion of HF exchange would considerably increase the gap relative to GGA. The comparison of PBE0 and HSE06 also reflect the fact that the energy gap is correctly reproduce by the short range nature of exact exchange. The VBM state lowering and CBM state lifting amount to 0.96 eV and 1.19 eV for PBE0 and 0.63 eV and 0.77 eV for HSE06. This trends is attributed to the HF admixed portion which reduce the self-energy of VBM and also raise the CBM. Using above methods we calculated the energetic, electronic and structural properties of each vacancy type. Since the vacancy induced state

TABLE II: The magnitude of vacancy neighbors outward relaxation in \AA for PBE0 and HSE06 are listed. The relative comparison shows lower relaxation of fully and half occupied vacancy levels(due to bounded electron to defect center) in hybrid functionals than GGA.

Ti-O	V_O^0	V_O^+	V_O^{2+}
GGA	1.128	1.151	1.127
PBE0	1.014	1.120	1.042
HSE06	1.000	1.121	1.009

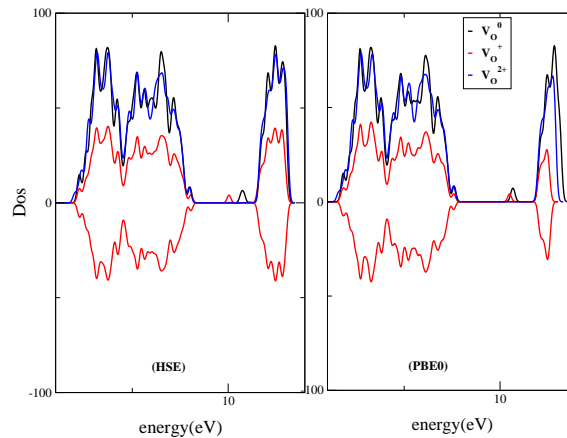


FIG. 9: Both HSE06 and PBE0 are successful in giving the neutral and singly ionized vacancies below CBM . HSE06 band gap is coincide with experimental gap and also the defect state is in closer agreement with experimental values and Ref²⁴.

are made from the three Ti atoms surrounding the vacancy , their relaxation magnitude is determinant to the positioning of vacancy states in the band structure. Table. II represent the distances of vacancy neighbors for GGA, PBE0 and HSE06.

It is obvious that in PBE0 and HSE06 the outward relaxation for V_O^0 and V_O^+ that have bounded electrons to vacancy center is relatively small compared to GGA while bigger outward relaxation is observed for V_O^{2+} than GGA analogous due to having no bounded electron. Having earned the amount of vacancy relaxation, we are able to interpret the obtained states in the gap as shown in Fig.9.

Upon introducing oxygen vacancy , its neighbors relax in order to reinforce their bonding with the rest of the lattice and results in less overlap between three Ti atoms and shift the vacancy state up. On the other hand if the vacancy center has bounded electrons it

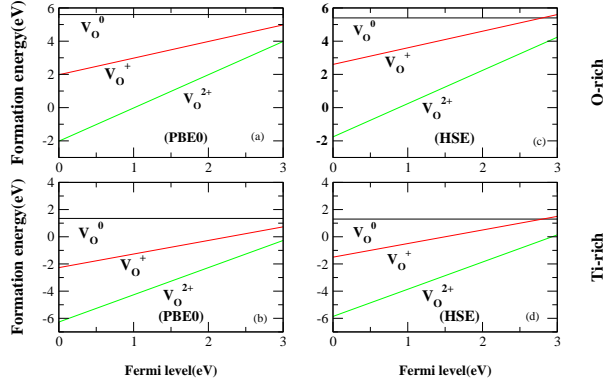


FIG. 10: The diagram of formation energy with Fermi energy variation is depicted for PBE0 and HSE06 hybrid functional for O-rich and Ti-rich conditions. Both functionals give the V_O^{2+} the stable vacancy with Fermi energy change and transition level $\epsilon(2+/0)$ is approximately within ~ 1 eV above conduction band minimum.

resist against outward relaxation since it gives unstable energetic picture. Hence balance of these two competitive factors determine the position of vacancy states. From the table II, it evidences that HSE06 and PBE0 show less outward relaxation than GGA for V_O^0 and V_O^+ while the situation is reversed for V_O^{2+} which give raise to the V_O^0 and V_O^+ levels 1.12 and 1.25 eV for PBE0 and 0.80 and 1.40 eV for HSE06 below CBM . Comparing V_O states for neutral and singly ionized charged vacancy in PBE0 and HSE06 indicate that energy shift of V_O^0 state is more than V_O^+ due to the presence of short part of exact exchange. Finally we address the extrapolated formation energy at O-rich and Ti-rich limit as shown in Fig. 10. The formation energy of V_O^{2+} is fairly low compared to V_O^+ and V_O^0 in terms of Fermi energy variation in the gap . The reason lies in the fact that these hybrid functionals lower the VBM level considerably lead to lowest formation energies(with no electron bounded to vacancy) and therefore the charge transition level lies above the gap . Our results for formation energy and $\epsilon(2+/0)$ is closed to HSE results of Ref.²⁴ . This implies that both V_O^0 and V_O^+ have always higher formation energy than V_O^{2+} make it only possible stable charged state of oxygen vacancy. This behavior is exactly same in both O-rich and Ti-rich regime except that the formation energies in Ti-rich are much lower than O-rich. Accordingly, this observation is mainly consistent with experimental measurement suggest conductivity reduction with increase of oxygen partial pressure²⁷.

IV. SUMMARY

In conclusion, we studied the problem of oxygen vacancies in viewpoint of gap correction method. With the application combined GW correction and $GGA+U$ starting point referred as $GW@GGA+U$, we found that the quasi particle energies shows different U -dependence traced back to their character and occupancy.. Additionally, we found that application of G_0W_0 depends on the starting point . It also fails to predict the vacancy state inside the gap contrary to the experimental findings. Alternatively , we employed hybrid functional PBE0 and HSE06 in which they are able to truly predict the neutral and singly ionized vacancies in the energy gap . However they gives raise to stable energetic picture of doubly ionized vacancy as a function of Fermi energy variation within the gap and transition level $\epsilon(2 + /0)$ about 0.6 eV and 0.8 eV for PBE0 and HSE06 above CBM reflect shallow n-type conductivity features of V_O .

V. ACKNOWLEDGMENT

This work was supported partially by the Vice Chancellor for Research Affairs of Isfahan University of Technology and ICTP Affiliated Center. A.Kazempour gratefully acknowledge fruitful discussions with M. Scheffler, S. Levchenko and P.Rinke. A. Kazempour appreciate FHI Institute der Max Plank Gesellschaft for financial support and computation resources during his visit.

¹ A. Fujishima and K. Honda, Nature(London). **238**, 37 (1972).

² R. West, R. Shirley, M. Kraft, C. Goldsmith, and W. Green, Gombust, Flame. **156**, 1764 (2009).

³ P. Kofstad, *Nonstoichiometry Diffusion and Electrical conductivity in Binary metal oxides* (Wiley, New York, 1972), 1st ed.

⁴ P. Kofstad, J. Phys. Chem. Solids. **23**, 1579 (1962).

⁵ J. Chen, L.B.Lin, and F. Q. Jing, J. Phys. Chem. Solids **62**, 1257 (2001).

⁶ E. Cho, S. Han, H. S. Ahn, K. R. Lee, S. K. Kim, and C. S. Hwang, Phys. Rev. B **73**, 193202 (2006).

⁷ M. Ramamoorthy, R. D. King-Smith, and D. Vanderbilt, Phys. Rev. B **49**, 7709 (1994).

- ⁸ S.-G. Park, B. MAgyari-Kope, and Y. Nishi, Phys. Rev. B **82**, 115109 (2010).
- ⁹ M. S. Hybertsen and S. G. Louie, Phys. Rev. B. **34**, 8 (1986).
- ¹⁰ A. Yamasaki and T. Fujishima, Phys. Rev. B. **66**, 245108 (2002).
- ¹¹ K. B. J. P. Perdew and M. Ernzerhof, Phys. Rev. Lett. **77**, 3865 (1996).
- ¹² QUANTUM-ESPRESSO is a community project for high-quality quantum-simulation software, based on density-functional theory, and coordinated by Paolo Giannozzi. See <http://www.quantum-espresso.org> and <http://www.pwscf.org>.
- ¹³ L. Hedin, Phys. Rev. **139**, A796 (1965).
- ¹⁴ F. Aryasetiawan and O. Gunnarsson, Rep. Prog. Phys. **61**, 237 (1998).
- ¹⁵ L.Martin-Samos and G. Bussi, Comput.Phys.Commun. **180**, 1416 (2009).
- ¹⁶ G. Makov and M. C. Payne, Phys. Rev. B. **51**, 7 (1994).
- ¹⁷ F. A. V. I. Anisimov and A. Lichtentein, J. Phys. Condens. Mater **9**, 767 (1997).
- ¹⁸ F. F. F. Bechstedt and G. Kresse, Phys. Status. Solidi. B **246**, 1877 (2009).
- ¹⁹ H. Jiang, R. Gomez-abel, P. Rinke, and M. Scheffler, Phys. Rev. Lett. **102**, 126403 (2009).
- ²⁰ H. Jiang, R. Gomez-abel, P. Rinke, and M. Scheffler, Phys. Rev. B. **82**, 045108 (2010).
- ²¹ K. M. Glassford and J. R. Chelikowsky, Phys. Rev. B. **46**, 1284 (1992).
- ²² P.Rinke, A. Janotti, M. Scheffler, and C. G. V. de Walle, Phys. Rev. Lett. **102**, 026402 (2009).
- ²³ S. Kummel and L. Kronik, Rev. Mod. Phys **80**, 3 (2008).
- ²⁴ A. Janotti, J. B. Varley, P. Rinke, N. Umezawa, G. Kresse, and C. G. V. de Walle, Phys. Rev. B **81**, 085212 (2010).
- ²⁵ J. Heyd and G. Scuseria, J. Chem. Phys **120**, 16 (2004).
- ²⁶ G. S. J. Heyd, J. E. Peralta and R. Martin, J. Chem. Phys. **123**, 174101 (2005).
- ²⁷ J. Moser, R. N. Blumenthal, and D. H. whitmore, J. Am. Ceram. Soc **48**, 384 (1965).